



PERFORMANCES OF DIRECT REACTIVE POWER CONTROL TECHNIQUE APPLIED TO THREE LEVEL-INVERTER UNDER RANDOM BEHAVIOR OF WIND SPEED

SALAH TAMALOUZT

Key words: Grid connected wind turbine conversion, Random behavior wind speed, Pitch angle control, Doubly fed induction generator, Direct torque and reactive power control, Fuzzy logic control, Three-level inverter.

A doubly fed induction generator (DFIG) driven by a variable speed wind turbine (WT) is presented in this paper. The DFIG is supplied via a three-level inverter in its rotor, and controlled with a flexible algorithm based on fuzzy logic control (FLC) combined with the direct torque (DTC), getting the direct reactive power control (DRPC) technique, thereby enjoying the benefits of both at same time. The aim of this contribution is to analyze the performances and robustness of the proposed control technique, which is applied to a three-level inverter. Indeed, the main objectives are to obtain at the generator output (AC) sine waveforms signals with a low total harmonic distortion (THD), as well as minimum output voltages ripples, regardless of the variation of the wind speed, as well as, the possibility of energy management, the active and reactive powers control by the DFIG, and the usefulness of this machine as a local reactive power compensator. Some constraints are taken in to account to reflect the real operation of a wind driven, such as the randomness behavior of the wind speed allowing the three operation modes of the DFIG, i.e. sub, super and synchronous. Such operation is carried out with a successive and continuous manner, with a particular focus on synchronous and overspeed modes. The captured wind power is optimized to extract the maximum power using the appropriate maximum power point tracking (MPPT) algorithm, below a nominal turbine speed. We will be acting on the pitch angle control, beyond the nominal turbine speed, whereas the power extraction maximization amounts to regulate the power produced at its rate value. The simulation tests are performed under Matlab/Simulink and the results show the effectiveness of the control strategy that leads to better performances of the system.

1. INTRODUCTION

Among the most-effective systems available to generate electricity, mention may be made of the wind power generation systems. However, in the case of grid connected structure, different electrical generators can be used. Whilst the DFIG remains widely used, due to the potential of delivering high yields in regard to energy production and allowing the independent control of active and reactive power generation without using capacitors for reactive power control [1]. In addition, the main advantage of this generator is the size of the power electronic converters that are smaller than those of conventional full-size stator converters. In the aim to develop a quiet, efficient, and economical micro-grid connected wind energy conversions, several techniques are proposed in the literature [2–15]. One competitive control technique is a direct torque control because of its numerous advantages as a simpler structure, lower machine parameters dependency, high dynamic and steady state performances. Many research works have already been done in this context [7–12]. Nevertheless, the combination of the WT-DFIG advantages and those of DTC applied to a three level-inverter, have not been reported in the three operation modes of the DFIG (sub, super and synchronous mode) in successive and continuous manner. In addition, the synchronous operation mode of the DFIG can take a considerable time interval, so that its study becomes a necessity, especially, if we want to take into account the randomness behavior of the wind speed, which is not well be reported in the literature. However, in [9–12], these modes were studied in a successive and continuous manner, but in the references [9–11], the study was done under a fixed wind speed in each mode. Except in [12], which has been developed in a general and superficial way.

While the real interests, and the benefits of the operation and use of the DFIG as well as the operation of the direct reactive power control technique, applied to multilevel inverter are not addressed.

In the field of control systems, it is well known that emerging control techniques such as fuzzy logic controller (FLC) are a good solution for complex systems where the models are unknown or in cases of a lack data in their parameters. In addition, they are easy to implement. The applications of FLC in renewable energy systems are reported in literature [12–15]; They showed a remarkable flexibility. These latter prompted us to the combination of this techniques and the DTC, getting the direct reactive power control (DRPC) technique, thereby enjoying the benefits of both at same time.

The structures based on multi-level inverters improve the efficiency maximize the power delivered to the load. A multilevel inverter has several advantages over a conventional two-level inverter that uses high switching frequency pulse width modulation (PWM). Multilevel inverters continue to receive more and more attention because of their high voltage operation capability, low switching losses, high efficiency and low output of electro magnetic interference. Multilevel converters not only can generate the output voltages with very low distortion, but also can reduce the dv/dt stresses; therefore, electromagnetic compatibility problems can be reduced. They're can operate at both fundamental switching frequency and high switching frequency PWM [16–18].

The DRPC application for a multilevel inverter was never mentioned in the literature, especially by taking into account the randomness nature of wind and its sudden changes. Knowing that the both main handicaps of control techniques can be summed up in their pursuit of references

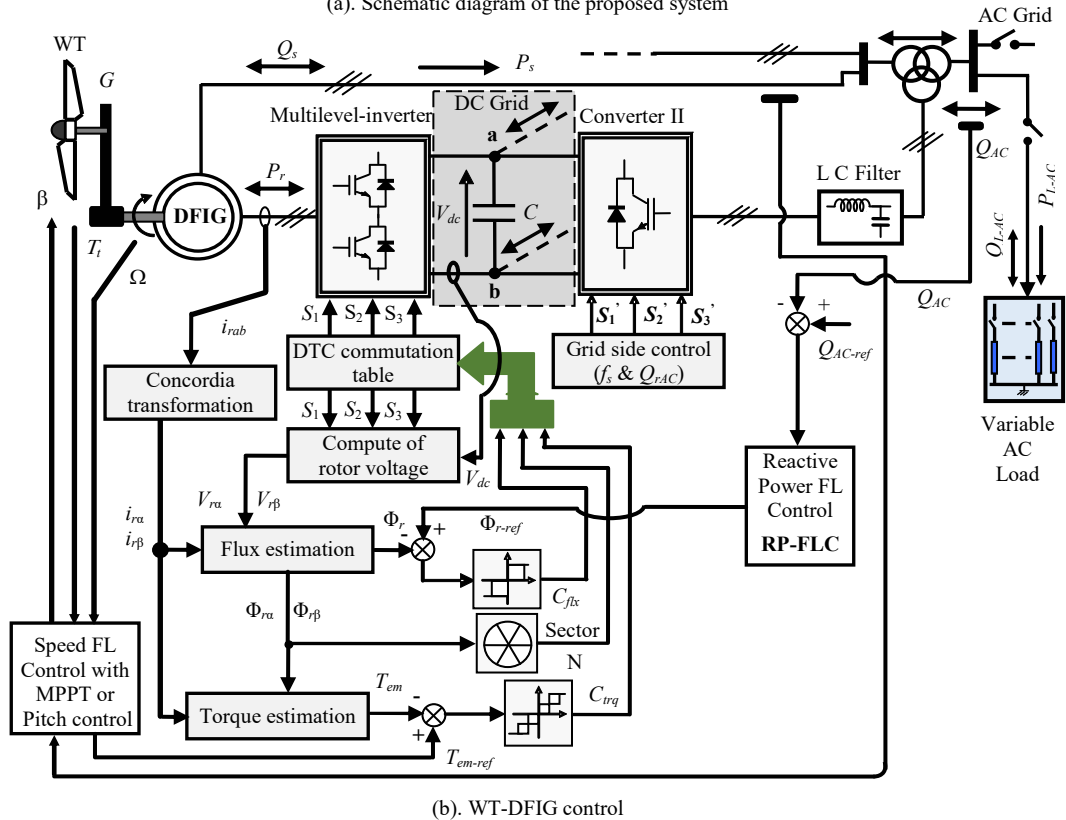
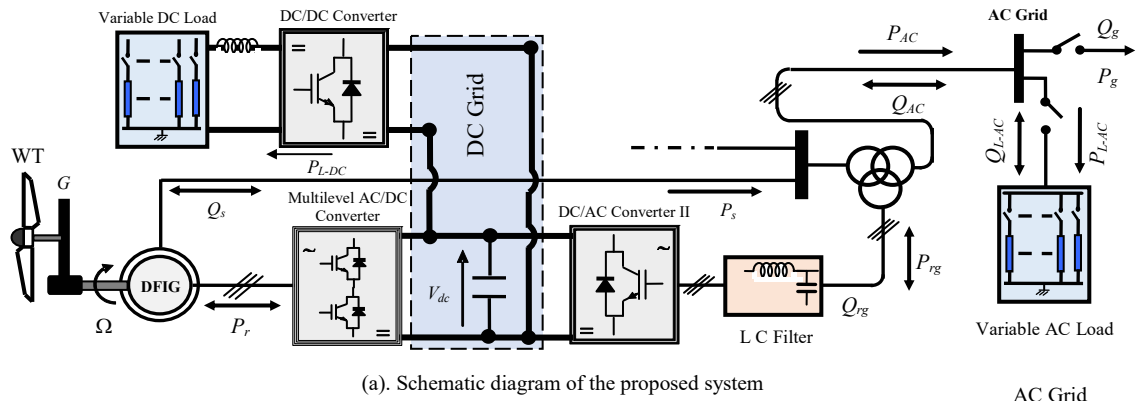


Fig. 1– Global control scheme.

to abrupt changes, and their robustness to external disturbances. In this context, the main objectives of this paper are to analyze the performances and the robustness of the DRPC technique, applied to a WT-DFIG supplied via a three level-inverter, taking into account the randomness variations of wind speed, allowing the DFIG operation in three modes, with a particular focus at two operating synchronous and overspeed modes. While taking into account the main advantage of the DFIG with its converter. In addition, the insertion of a three-level inverter to the DFIG will allow the generated signals of very acceptable waves forms and very low THD. Moreover, the quality and performances of this technique are examined in a manner to reproduce some constraints that reflect the real operation of the wind, such as the stochastic nature of wind speed in the most interesting operating zones of WT characteristics.

In this paper, the studied system is presented. Then, the models used to simulate the WT operation, the DFIG with its converter and the MPPT algorithms to maximize the generated power, below a nominal turbine speed are introduced. Beyond the nominal turbine speed, maintaining

constant the reference speed is necessary. When the nominal power is reached, power extraction maximization amounts to regulate the generated power at its rate value, acting on the blades pitch angle, *i.e.* Pitch Angle Control. The control of the reactive power is obtained by acting on the rotor flux, whereas the electromagnetic torque ensures the command of the generated active power. The proposed control strategy is based on direct torque control combined with the fuzzy logic technique, getting the direct reactive power control. The effectiveness and the performances of the proposed system are validated by simulation using MATLAB/ SIMULINK.

2. PROPOSED SYSTEM DESCRIPTION

The overall system is given in the Fig. 1. It is based on a DFIG dedicated to a wind turbine partially interfaced with the grid, via an indirect frequency converter (ac/ac). This latter consists of two converters separated by an intermediate dc bus, serving as a dc grid. The first converter (I) is a three level-inverter connected to the rotor of this machine, and controlled by the proposed control (DRPC).

Whilst, the connection to the ac grid is provided via a second converter (II) controlled so as to maintain its output at an unit power factor operations and to guarantee sinusoidal signals with a constant frequency of 50 Hz.

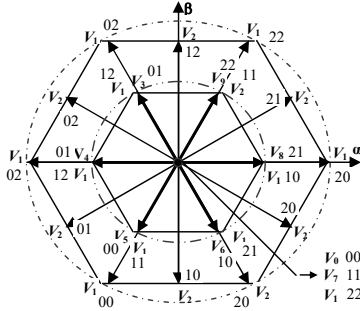


Fig. 2 – Space voltage vector diagram (case of twelve sectors with the null voltages vectors)

3. DESCRIPTION OF THE DIRECT TORQUE CONTROL OF THE THREE LEVEL INVERTER

The wind turbine controller objectives depend on the operating zone, as described in [1].

The DTC is based on the regulation of the rotor flux magnitude and the value of the machine electromagnetic torque, where the rotor flux magnitude is estimated from its components along the α and β axes [1, 11]:

$$\begin{cases} \Phi_{r\alpha}(t) = \int_0^t (v_{r\alpha} - R_r i_{r\alpha}) dt \\ \Phi_{r\beta}(t) = \int_0^t (v_{r\beta} - R_r i_{r\beta}) dt \end{cases} \quad (1)$$

The electromagnetic torque is given in [1, 11] by the following expression:

$$T_{em} = p(\Phi_{r\alpha} i_{r\beta} - \Phi_{r\beta} i_{r\alpha}). \quad (2)$$

To analyze the potential generated by this three states inverter, every arm is schematized by three switches which permit to independently connect the stator inputs to the source potentials (represented by $V_{dc}/2$, 0 and $-V_{dc}/2$).

By making a transformation into $\alpha\beta$ (or dq) frames, a resulting voltage vector is defined and associated to the

spatial position of the stator flux. Then, the different states number of this vector is 19, since some of the 27 possible combinations produce the same voltage vector, Fig. 2.

The space voltage vector diagram, for the three-level inverter, is divided into twelve sectors by using the diagonal between the adjacent medium and long vector.

According to the errors of torque and the stator flux linkage, the optimal vector is selected, from all 19 different available vectors, Fig. 2.

To implement the Direct Torque Control of DFIG is directly established through the selection of the appropriate rotor vector to be applied by the three-level inverter NPC structure. To do that, in first state, the estimated values of rotor flux and electromagnetic torque are compared to their respective references through hysteresis controller.

The elaboration of the control structure is based on the hysteresis controller output relating to the variable flux (C_{flx}) and the variable torque (C_{trq}) and the sector N corresponding to the rotor flux vector position.

We can consider the case where rotor flux is achieved by using three-level hysteresis comparator and electromagnetic torque by using 5-level hysteresis. The inverter state is considered as high if the output of torque comparator is high or equal to two. Otherwise, the state is low.

For the control of the electromagnetic torque, we have used a five-level hysteresis comparator, which permits to have the two senses of machine rotation. The output of this corrector is represented by a Boolean variable C_{trq} indicating directly if the amplitude of the torque must be increased, decreased or maintained constant ($C_{trq} = 1, 2, 0, -2, -1$), as modeled by equation (3).

For rotor flux control, a three-level hysteresis comparator are used. So, we can easily control and maintain the flux vector Φ_r in hysteresis bound. The output of this corrector is represented by a Boolean variable C_{flx} which indicates directly if the amplitude of flux must be increased ($C_{flx} = 1$), decreased ($C_{flx} = -1$) or maintained constant ($C_{flx} = 0$) so as to maintain: $|\Phi_{r_ref} - \Phi_r| \leq \Delta\phi_r$, as described by equation (4).

Table 1 represents the commutation table, is considered one of the solutions adapted to choose the optimal selected voltage vector for each sector. In this case, rotor flux and torque are achieved by using respectively three levels and five levels hysteresis comparators.

Table 1

DTC Commutation table of the three-level inverter

C_{flx}	C_{trq}	N											
		1	2	3	4	5	6	7	8	9	10	11	12
+1	+2	V_{21}	V_{16}	V_{22}	V_{17}	V_{23}	V_{18}	V_{24}	V_{19}	V_{25}	V_{20}	V_{26}	V_{15}
	+1	V_{21}	V_2	V_{22}	V_3	V_{23}	V_4	V_{24}	V_5	V_{25}	V_6	V_{26}	V_1
	0	Zero vector											
	-1	V_{26}	V_1	V_{21}	V_2	V_{22}	V_3	V_{23}	V_4	V_{24}	V_5	V_{25}	V_6
	-2	V_{26}	V_{15}	V_{21}	V_{16}	V_{22}	V_{17}	V_{23}	V_{18}	V_{24}	V_{19}	V_{25}	V_{20}
-1	+2	V_{17}	V_{23}	V_{18}	V_{24}	V_{19}	V_{25}	V_{20}	V_{26}	V_{15}	V_{21}	V_{16}	V_{22}
	+1	V_3	V_{23}	V_4	V_{24}	V_5	V_{25}	V_6	V_{26}	V_1	V_{21}	V_2	V_{22}
	0	Zero vector											
	-1	V_5	V_{25}	V_6	V_{26}	V_1	V_{21}	V_2	V_{22}	V_3	V_{23}	V_4	V_{24}
	-2	V_{19}	V_{25}	V_{20}	V_{26}	V_{15}	V_{21}	V_{16}	V_{22}	V_{17}	V_{23}	V_{18}	V_{24}
0	+2	V_{22}	V_{17}	V_{23}	V_{18}	V_{24}	V_{19}	V_{25}	V_{20}	V_{26}	V_{15}	V_{21}	V_{16}
	+1	V_{22}	V_3	V_{23}	V_4	V_{24}	V_5	V_{25}	V_6	V_{26}	V_1	V_{21}	V_2
	0	Zero vector											
	-1	V_{25}	V_6	V_{26}	V_1	V_{21}	V_2	V_{22}	V_3	V_{23}	V_4	V_{24}	V_5
	-2	V_{25}	V_{20}	V_{26}	V_{15}	V_{21}	V_{16}	V_{22}	V_{17}	V_{23}	V_{18}	V_{24}	V_{19}

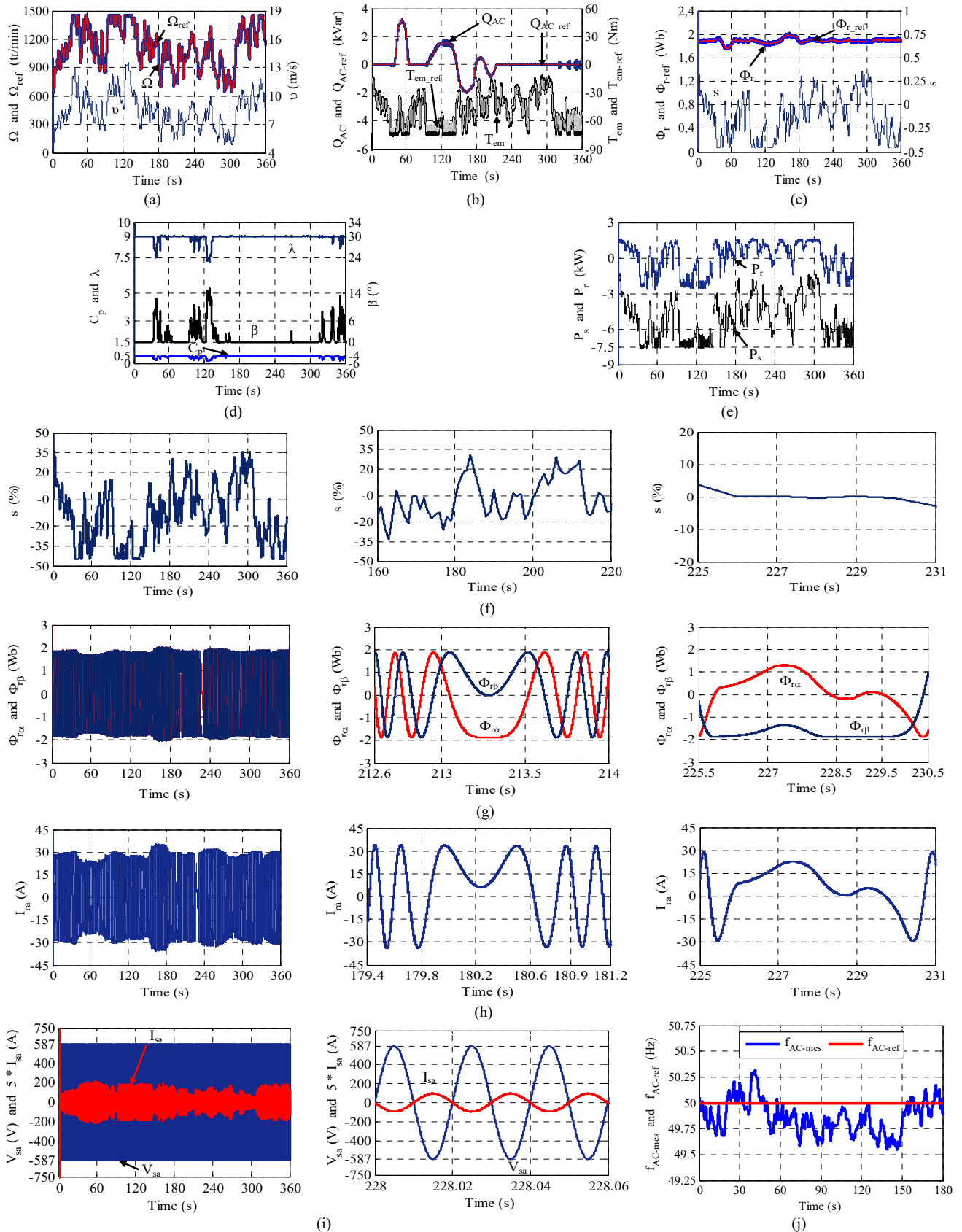


Fig. 3 – Waveforms of the simulation results for a variable wind speed and a reactive power requirements profiles: (a) - Ω , Ω_{ref} and v ; (b) - Q_{AC} , Q_{AC-ref} , T_{em} and T_{em-ref} ; (c) - Φ_r , Φ_{r-ref} and s ; (d) - β , λ and C_p ; (e) - P_r and P_s ; (f) - s and its zoom for two intervals; (g) - $\Phi_{r\alpha}$, $\Phi_{r\beta}$ and their zooms; (h) - $I_{r\alpha}$ and its zoom for two intervals; (i) - I_{sa} and its zoom for the synchronous mode; (j) - Zoom of the frequency current supplied to the grid and its reference.

In analyzing the effect of each available voltage vector, it can be seen that the vector affects the torque and flux linkage with the variation of the module and direction of the selected vector.

The nulls voltages vectors (V_0 , V_7 and V_{14}) are chosen alternately, so as to minimize the number of commutations in the arms of the inverter [16].

$$\left\{ \begin{array}{ll}
\text{If } \Delta tr > \varepsilon_{tr_2} & \text{Then; } C_{trq} = +2 \\
\text{If } -\varepsilon_{tr_1} \leq \Delta tr \leq \varepsilon_{tr_2} & \& \frac{\Delta tr}{dt} > 0 \text{ Then; } C_{trq} = +1 \\
\text{If } -\varepsilon_{tr_1} \leq \Delta tr \leq \varepsilon_{tr_2} & \& \frac{\Delta tr}{dt} < 0 \text{ Then; } C_{trq} = +2 \\
\text{If } 0 < \Delta tr \leq \varepsilon_{tr_1} & \& \frac{\Delta tr}{dt} > 0 \text{ Then; } C_{trq} = 0 \\
\text{If } 0 < \Delta tr \leq \varepsilon_{tr_1} & \& \frac{\Delta tr}{dt} < 0 \text{ Then; } C_{trq} = +1 \\
\text{If } -\varepsilon_{tr_1} \leq \Delta tr \leq 0 & \& \frac{\Delta tr}{dt} > 0 \text{ Then; } C_{trq} = -1 \\
\text{If } -\varepsilon_{tr_1} \leq \Delta tr \leq 0 & \& \frac{\Delta tr}{dt} > 0 \text{ Then; } C_{trq} = 0 \\
\text{If } -\varepsilon_{tr_2} \leq \Delta tr \leq -\varepsilon_{tr_1} & \& \frac{\Delta tr}{dt} > 0 \text{ Then; } C_{trq} = -2 \\
\text{If } -\varepsilon_{tr_2} \leq \Delta tr \leq -\varepsilon_{tr_1} & \& \frac{\Delta tr}{dt} > 0 \text{ Then; } C_{trq} = -1 \\
\text{If } \Delta tr < -\varepsilon_{tr_2} & \text{Then; } C_{trq} = -2.
\end{array} \right. \quad (3)$$

$$\left\{ \begin{array}{ll}
\text{If } \Delta \varphi_r > \varepsilon_{f_{lx}} & \text{Then; } C_{f_{lx}} = +1 \\
\text{If } 0 \leq \Delta \varphi_r \leq \varepsilon_{f_{lx}} & \& \frac{\Delta \varphi_r}{dt} > 0 \text{ Then; } C_{f_{lx}} = 0 \\
\text{If } 0 \leq \Delta \varphi_r \leq \varepsilon_{f_{lx}} & \& \frac{\Delta \varphi_r}{dt} < 0 \text{ Then; } C_{f_{lx}} = +1 \\
\text{If } -\varepsilon_{f_{lx}} < \Delta \varphi_r < 0 & \& \frac{\Delta \varphi_r}{dt} > 0 \text{ Then; } C_{f_{lx}} = -1 \\
\text{If } -\varepsilon_{f_{lx}} < \Delta \varphi_r < 0 & \& \frac{\Delta \varphi_r}{dt} < 0 \text{ Then; } C_{f_{lx}} = 0 \\
\text{If } \Delta \varphi_r < -\varepsilon_{f_{lx}} & \text{Then; } C_{f_{lx}} = -1.
\end{array} \right. \quad (4)$$

The detailed control of both external loops are given in [1, 12]. Knowing that these last are the reactive power and the mechanical speed loops.

The compensation of the reactive power exchanged between the proposed system and the busbar from the ac side (Q_{rg}) is provided by the DFIG. Knowing that the reactive power at the dc/ac converter II output is forced to zero, i.e. operating at unity power factor [1].

4. SIMULATION RESULTS

The proposed system is tested under the Matlab/Simulink environment. The simulation parameters are given in [1, 19]. The total hourly averages of the weather data in terms of wind speed and the reactive power requirements profiles, up to 360 seconds are shown in Figs. 3a and b. The DFIG mechanical speed and the randomness wind speed profile are presented in Fig. 3a.

The pursuit of the references is shown by the waveforms of the mechanical speed, electromagnetic torque and the involved reactive power with the rotor flux magnitude, as illustrated respectively in Figs. 3 a, b and c. The electromagnetic torque follows its reference, and varies as a result of the wind speed profile to maximize the generated active power in the zones I and II, of the WT characteristic. While, in the zone III, the electromagnetic torque is kept constant to maintain the constant produced power.

Therefore, the magnitude of the rotor flux is kept at its reference and varies according to the involved reactive power, as shown in Fig. 3c. Then, the WT-DFIG is used in optimal way, where the possibility of using the DFIG to control and manage the active-reactive powers is confirmed. Hence, these results confirm the good performances and the robustness of the proposed DRPC

control. In addition, we can clearly see that the torque ripples are decreased by about 65 % compared to the results given in reference [1, 11, 12].

Figure 3d illustrates the β , λ and C_p . When the power reached its maximum value, the pitch angle control is activated, as presented in Fig. 3e. Therefore, the mechanical speed is kept constant, at its limit value. Then, the electromagnetic torque is maintained constant. However, in the regions I and II, the generated active power is maximized by the MPPT algorithm.

Figure 3e shows all the exchanged powers between the grid and WT-DFIG; The rotor power (P_r) changes its direction, marked by its sign, according the generator slip, this reflects two operating modes, subsynchronous and supersynchronous, as presented in Fig. 3f.

The two axes rotor fluxes waveforms ($\Phi_{r\alpha}$ and $\Phi_{r\beta}$) are shown in Fig. 3g, with a sinusoidal behavior in the subsynchronous and supersynchronous modes. However, in the synchronous mode the fluxes have a continuous form. Also, this mode is illustrated by a direct form of the rotor phase currents as shown in Figs. 3h. In this figure, we illustrate the sinusoidal evolution of the phase's rotor current in the sub and supersynchronous operation modes. The randomness evolution of the rotor current magnitude is related to the electromagnetic torque variations and its pulsation is depending on the slip variations.

Besides, the signal quality and its waveform, as shown in Figure 3h, illustrate good performances of the current waveform. Which has repercussions on the stator power generated by the DFIG to the ac grid. Knowing that minimizing the harmonics at the rotor supply level is equivalent to improving the quality of the wave generated by the system. The stator current keeps a sinusoidal form throughout of the three operating modes with a constant frequency of 50 Hz, along with, a variable amplitude, as shown in Figs. 3i and j.

The proposed control strategy, DRPC associated to the three-level inverter, the waveforms of the stator currents supplying the ac grid, are significantly improved compared to that of the two-level inverter, as studied in [1, 12], with a low total harmonic distortion (THD), whereas largely below the limits imposed by IEEE std 519, as illustrated in Figs. 4a, b and c. Also, with a almost constant frequency of 50 Hz Fig. 3j. This confirms a better quality of energy generated in the ac grid.

5. CONCLUSION

The performances and robustness of the DRPC have been presented in this paper. This technique is applied a three-level inverter to control the active and the reactive powers of DFIG. While taking into account the mains advantages of this generator associated with its converter, that are: a management system of active energy and, a reactive power local compensator. In addition, the quality and performances of this technique are examined in a manner to reproduce some constraints that reflect the real behavior of the wind. Thus, the randomness behavior of the wind speed allowed the utilization of the machine in its different operation modes. Attention is made on the dynamic performance of DRPC. The effectiveness of the proposed scheme control is demonstrated by simulation using Matlab/ Simulink.

The obtained results show clearly the good performances of the proposed system control in the different operation modes, in terms of pursuit of the references or the robustness. Thus, the significant

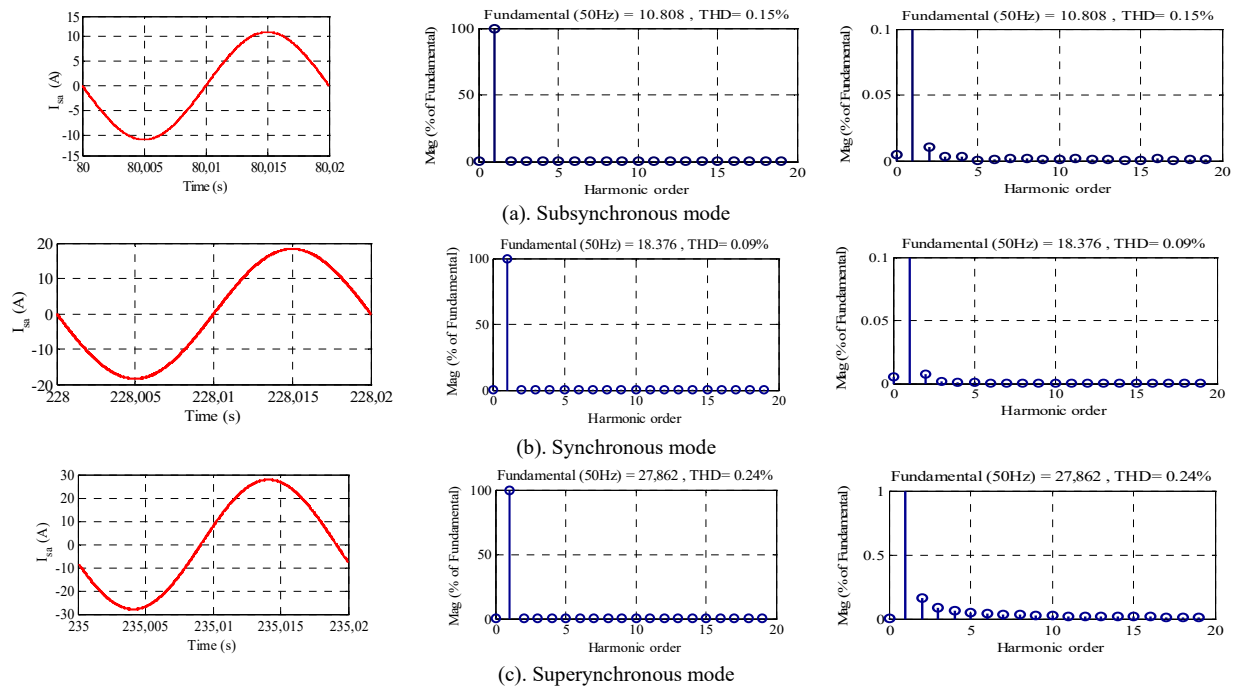


Fig. 4 – Waveforms of the generated phase current (stator current) and its harmonic spectrum, for three operation modes.

performances of the DFIG control under wind randomness variations. This allows us to confirm the robustness behavior and the satisfactory performances of the proposed technique. Also, they justify the utility of the DFIG in the possibility of management, and the control of the reactive and active powers. This leads to use the DFIG as a reactive power local compensator.

The simulation results show that the application of the proposed control technique, significantly improves the performance of the conversion system, which amounts to reduce the total harmonic distortion in the currents waves and the torque oscillations. These results indicate that the combination of the advantages of DTC combined with the FLC gives a better answer to the requirements of the grid.

The overall control based on DRPC has significantly improved the performances of the overall system under wind randomness variation. In addition to the contribution of this control technique, the three-level inverter inserted in the DFIG rotor has also participated to improve the power quality injected into the ac grid.

Received on January 21, 2018

REFERENCES

1. S. Tamalouzt, N. Benyahia, T. Rekioua, D. Rekioua and R. Abdessemed, *Performances analysis of WT-DFIG with PV and fuel cell hybrid power sources system associated with hydrogen storage hybrid energy system*, International Journal of Hydrogen Energy, **41**, 45, pp. 21006-21021 (2016).
2. K. C. Wong, S. L. Ho, K. W. E. Cheng, *Direct torque control of a doubly-fed induction generator with space vector modulation*, Elec. Pow. Comp. and Syst., **36**, 12, pp. 1337-1350 (2008).
3. M. Rahimi, M. Parniani, *Dynamic behavior analysis of doubly-fed induction generator wind turbines, the influence of rotor and speed controller parameters*, Int. J. of Elec. Pow. and Energy Syst., **32**, 5, pp. 464-477 (2010).
4. K. Kerrouche, A. Mezouar, K. Belgacem, *Decoupled control of doubly fed induction generator by vector control for wind energy conversion system*, Energy Procedia, **42**, pp. 239-248 (2013).
5. M. Adjoudj, M. Abid, A. Aissaoui, Y. Ramdani, H. Bounoua, *Sliding mode control of a doubly fed induction generator for wind turbines*, Rev. Roum. Sci. Techn. – Electrotechn. et Energ., **56**, 1, pp. 15-24 (2011).
6. A. Abdelfetteh, M. Abid, *Hybrid fuzzy sliding mode control of a doubly fed induction generator in wind turbines*, Rev. Roum. Sci. Techn. – Electrotechn. et Energ., **57**, 4, pp. 15-24 (2012).
7. J. Arbi, M. J. Ben Ghorbal, I. Slama-Belkhdja, L. Charaabi, *Direct virtual torque control for doubly fed induction generator grid connection*, IEEE Trans. on Ind. Electron., **56**, 10, pp. 4163-4173 (2009).
8. J. Ben Alaya, A. Khedher, M. F. Mimouni, *Speed-sensorless DFIG wind drive based on DTC using sliding mode rotor flux observer*, Int. J. of Renew. Energ. Res., **2**, 4, pp. 735-745 (2012).
9. A.F. Payam, M.N. Hashemnia, J. Faiz, *Robust DTC control of doubly fed induction machines based on input-output feedback linearization using recurrent neural networks*, Journal of Power Electronics (JPE), **11**, 5, pp. 719-725 (2011).
10. S. Tamalouzt, T. Rekioua, R. Abdessamed, K. Idjdarene, *Direct torque control of grid connected doubly fed induction generator for the wind energy conversion*, International Renewable Energy Congress IREC'2012, Sousse, Tunisia, pp. 1-6, Dec. 19-22, 2012.
11. S. Tamalouzt, K. Idjdarene, T. Rekioua, R. Abdessamed, *Direct Torque Control of Wind Turbine Driven Doubly Fed Induction Generator*, Rev. Roum. Sci. Techn. – Electrotechn. et Energ., **61**, 3, pp. 244–249 (2016).
12. S. Tamalouzt, T. Rekioua, R. Abdessemed, *Direct Torque and Reactive Power Control of Grid Connected Doubly Fed Induction Generator for the Wind Energy Conversion*, International Conference on Electrical Sciences and Technologies in Maghreb (CISTEM), Tunis, pp. 1-7, 3-6 Nov. 2014.
13. L. Suganthi, S. Iniyar, A. A. Samuel, *Applications of fuzzy logic in renewable energy systems—A review*, Renewable and Sustainable Energy Reviews, **48**, pp. 585-607 (2015).
14. S. Louarem, S. Belkhat, D. E. C. Belkhat, *A control method using PI/fuzzy controllers based DFIG in wind energy conversion system*, IEEE Grenoble Power Tech, pp. 1-6 (2013).
15. S. Meddouri, K. Idjdarene, L. Ferrarini, *Control of Autonomous Saturated Induction Generator Associated to a Flywheel Energy Storage System*, Rev. Roum. Sci. Techn. – Electrotechn. et Energ., **61**, 4, pp. 372–377 (2016).
16. A. Nami, J. Liang, F. Dijkhuizen, and G. D. Demetriades, *Modular multilevel converters for HVDC applications: Review on converter cells and functionalities*, IEEE Transactions on Power Electronics, **30**, 1, pp. 18-36 (2015).
17. A. Nami and F. Zare, *Multilevel Converters in Renewable Energy Systems*, Cooperstown, NY, USA: In-Tech, Jan. 2010.
18. A. Lega, *Multilevel Converters: Dual Two-Level Inverter Scheme*, Ph.D thesis in Electrical Engineering, University of Bologna, 2007, pp. 39-51.
19. R. S. Pena, R. J. Cardenas, G. M. Asher, J. C. Clare, *Vector controlled induction machines for stand-alone wind energy applications*, IEEE Ind. Appl. Conf., Rome, Italy, pp. 1409-1415, Oct. 08-12, 2000.